# Comprehensive study of Speed Control of Induction Motor using MOSFET Chopper and Inverter Based Slip Power Recovery Scheme

Abhishek Thakur*[1], Navneet Kumar*[2,] Geena Sharma*[3]
Abhishek Thakur- M.Tech Student, Navneet Kumar- M.Tech Student, Geena Sharma- H.O.D./Assistant Professor Electrical Engg. Deptt.
Abhishek Thakur*[1]- Electrical Engineering Deptt.
*BUEST Baddi University of Emerging Sciences and Technology Solan HP India

**Abstract—Speed control of slip ring induction motor (SRIM) has important aspect in adjustable speed drive applications. The power semiconductor technology has played a crucial role in the advancement of adjustable speed induction motor drives employing slip power recovery scheme (SPRS). For the narrow speed range, slip power is a fraction of the power rating of the induction motor, therefore, a lesser rating of converter and inverter certainly reduce size and cost of the drive. This paper presents the performance evaluation of MOSFET chopper and inverter controlled SPRS based IMD. The simulation model of IMD using MOSFET based buck-boost chopper and pulse width modulated voltage source inverter (PWMVSI) have been build up in MATLAB 2013b for performance evaluations. The performances of IMD have been investigated by taking in to account the parameters viz. power factor, efficiency and quality of supply in terms of total harmonic distortion (THD). The simulation results signify that the MOSFET chopper and PWMVSI controlled SPRS based IMD has higher power factor, efficiency and superior quality of supply with lesser THD in comparison of SPRS with SCR inverter control.**

***Keywords—chopper, efficiency, induction motor, power factor, slip power recovery scheme.***

## I. INTRODUCTION

About 70% of industrial loads are run by induction motor drives. ring induction motor (SRIM) are used in the industrial field where the drive operation is intermittent i.e. hoists, cranes, conveyers, and lifts because the slip power can be easily controlled by slip rings. The slip power recovery scheme (SPRS) controls the speed of SRIM by sending back the feedback power to the supply mains thereby improves the efficiency of the SRIM drive [1]. SRIM drive operates at limited speed range and has slip power a smaller part of motor power rating, hence low rating of converter and lower cost [2]. The researchers are drawing more interest in the field of renewable energy sources because of advancement in the static converters technology [3-4]. The major setback of SPRS has been found to be as i) poor power factor of the supply, ii) requirement of higher reactive power and iii) high harmonic components [5-6]. The existence of harmonic contents produced the distortion in the supply source. In literature number of methodologies [7] has been reported to improve the performances of the slip power recovery drive (SPRD). A methodology employing buck chopper has operated the inverter at most secure firing angle and decrease the reactive power consumption of inverter in this manner improve the power factor and efficiency of SRIM drive [8].

The different circuit configurations of PWM inverter and boost chopper have been utilized in the DC link of SPRS to control active and reactive power and also decreases the harmonics of rotor side [9, 10]. The utilization of boost/buck-boost chopper has replaced one of the insulated gate bipolar transistor (IGBT) converters from the rotor circuit side by silicon controlled rectifier (SCR) converter and decrease the cost of SPRS with the same performance indices of induction machine [11]. Theoretically the mathematical model has been drawn to evaluate the DC link of SPRD [12]. A twelve pulse SCR inverter with IGBT boost chopper has been exercised to enhance the power factor, while SPRD utilizing voltage source inverter (VSI) and boost chopper applying voltage control technique and current control technique decrease the total harmonic distortion (THD) of source and improved the power factor [13-15]. A SPRD system using buck converter and inverter with three PWM techniques in the intermediate circuit has been used with LC filter to decrease the harmonic contents of supply source [16]. The inverter configuration with step-down and step-up/down chopper has enhanced the power factor and efficiency of the SRIM drives and quality of power supply [17, 18].

## II. MATHEMATICAL MODELING OF SPRS

Mathematical modeling of conventional SPRS has been given in this subsection.

### *A.* Model of the conventional SPRS

In slip power recovery scheme shown in "Fig. 1,", the three-phase full-wave diode bridge rectifier connects to the rotor windings through slip rings, converts. A portion of slip power is converted in to DC by this rectifier and inverted into line frequency AC by a three-phase SCR inverter and feedback to the supply mains. The feedback power can be controlled by controlling the inverter emf $V_{d2}$, by changing the firing angle of the inverter. The DC link inductor $L_d$ has been provided to reduce ripples in DC link current $I_d$ and the transformer to match the voltages $V_{d1}$ and $V_{d2}$ by taking a suitable turn's ratio.

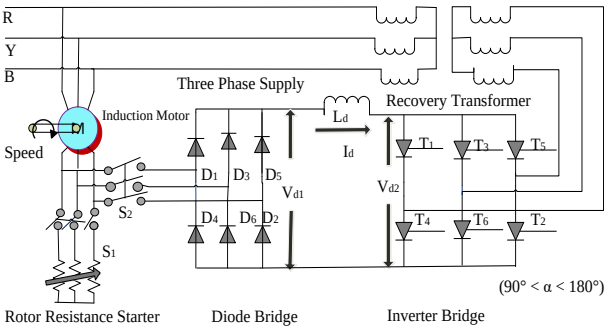

Fig. 1. Diagram of SPRS utilizing SCR Inverter

Avoiding stator and rotor drops the values of rectifier and inverter output voltages and the slip can be described by equation (1)-(3) below [19].

$$V_{d1} = \frac{3\sqrt{2}}{\pi} \times \frac{sV}{n} \Rightarrow 1.35 \times \frac{sV}{n} \quad (1)$$

$$V_{d2} = \frac{3\sqrt{2}}{\pi} \times \frac{V}{m} \cos\alpha \Rightarrow 1.35 \times \frac{V}{m} \cos\alpha \quad (2)$$

$$s = \frac{n}{m} |\cos\alpha| \quad (3)$$

where $V_{d1}$ and $V_{d2}$ are the diode bridge and inverter-bridge output voltages, $\alpha$ = the inverter firing angle, $m$ = the turns ratio of transformer from source to converter side, $n$ = the turns ratio of induction motor from stator to rotor side, $s$ = the slip, $V$ = the input voltage. Extreme value of $\alpha$ is confined to $165°$ for secure commutation of thyristors. The desired speed can be obtained with proper choice of $\alpha$ [19].

The equations for DC link current, air gap power, and electromagnetic torque are given by (3), (4), (5) and (10) below [18]

$$I_d = \frac{V_{d1} + V_{d2}}{2(sR_s^{'} + R_r) + R_d} \quad (4)$$

Neglecting copper loss

$$sP_g = |V_{d2}| I_d \Rightarrow 1.35 \times \frac{V}{m} \cos\alpha \times I_d \quad (5)$$

From equations (4) and (6)

$$P_g = 1.35 \frac{V}{n} \times I_d \quad (6)$$

$$P_m = (1-s) P_g = T_d \times \omega_r \quad (7)$$

$$\Rightarrow P_m = T_d \times \omega_m (1-s) \frac{2}{p} \quad (8)$$

The electromagnetic torque is given by

$$T_d = \frac{p}{2} \times \frac{P_g}{\omega_m} \quad (9)$$

From equations (7) and (10), electromagnetic torque can be written as

$$T_d = \left(\frac{p}{2}\right) \frac{1.35V}{n \times \omega_m} \times I_d \quad (10)$$

where, $I_{dc}$ = DC link current, $R_s^{'}$ = rotor side referred stator resistance to, $R_r$ = rotor resistance, $R_d$ = DC link inductor resistance, $P_g$ = air gap power, $T_d$ = electromagnetic torque, $P_m$ mechanical power at the shaft, $\omega_m$ and $\omega_r$ are the synch. speed and rotor speed in rad/sec, $p$ = no of poles [20].

Equation (11) pointed out that the torque is directly proportional to DC link current and the magnitude of which depends upon the voltage difference between the $V_{d1}$ and $V_{d2}$. Consequently, the torque speed curves of IMD are just about linear like separately excited DC motor for any particular value of inverter firing angle.

*B.* Proposed SPRS Model with MOSFET based Buck-Boost Chopper control technique

The setback of the conventional SPRS is high reactive power drawn from the source by the inverter when firing angle varies above 90°, which decreases power factor and quality of supply mains by increasing the THD. To avoid this problem the proposed scheme has utilized the buck-boost chopper control technique as shown by "Fig. 2," controlling the speed of the induction motor by duty ratio control at fixed value $\alpha$ taking minimum reactive power from the source. Therefore, this technique will reduce the reactive power consumption of the inverter thereby improves the power factor of the supply.

Taking in to consideration the DC link equivalent circuit of "Fig. 2," the DC voltage of inverter, slip and DC link current can be written as [18]

$$V_{d2} = 1.35 \left(\frac{\delta}{1-\delta}\right) \frac{V}{m} \cos\alpha \quad (12)$$

$$s = \frac{n}{m} \left(\frac{\delta}{1-\delta}\right) |cos\alpha| \quad (13)$$

$$I_d = \frac{V_{d1} - V_{d2}}{R_{dc}} \quad (14)$$

where, $\delta$ = duty ratio of chopper and $R_{dc}$ = the DC link circuit is resistance which can be expressed as [13]

$$R_{dc} = \left\{2R_s' + \frac{3(X_s' + X_r)}{\pi}\right\} s + R_r + R_d \quad (15)$$

Air gap power, motor torque, and power factor are given by

$$sP_g = |V_{d2}| I_d \Rightarrow P_g = \frac{|V_{d2}| I_d}{s} \quad (16)$$

$$T = \frac{P_g}{\omega_m} \Rightarrow \frac{|V_{d2}| I_d}{s\omega_m} \quad (17)$$

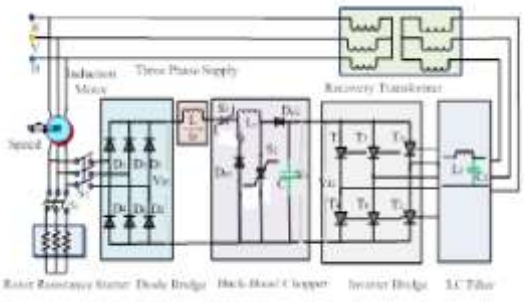

Fig. 2. Diagram of SPRS employing SCR Inverter and buck-boost chopper

$$cos\phi = \frac{(P_s - P_r)}{\sqrt{(P_s - P_r)^2 + (Q_s + Q_r)^2}} \quad (18)$$

where $X_s'$ = reactance of stator referred to rotor side and $X_r$ = reactance of rotor respectively. $P_s$ = active power and $Q_s$ = reactive power consumed by inverter and motor from the supply source. $P_r$ = active power recovered by inverter and $Q_r$ = reactive power taken/recovered by the inverter from the supply source and is written as

$$P_r = 1.35V \left(\frac{\delta}{1-\delta}\right) cos\alpha \times I_d \quad (19)$$

$$Q_r = 1.35V \left(\frac{\delta}{1-\delta}\right) sin\alpha \times I_d \quad (20)$$

Equation (20) shows that the reactive power drawn from the source can be decreased by decreasing duty ratio keeping firing angle fixed which in turn increases the power factor as represented by equation (18). Hence the proposed scheme improves the power factor.

## III. Modeling and Simulation of SPRS

SPRS employing the SCR inverter as shown in "Fig. 3," has been simulated in the MATLAB 2013b. The measurement blocks like Fourier block, and discrete block have been used to measure the speed, rms value of current, power factor of the current and the active and reactive power drawn from the

source. The model of IMD 2 hp, 415V, 50Hz, 1430 rpm has been simulated employing SCR inverter bridge. The model is running on MATLAB and different observations are plotted as shown in "Fig. 5,"-"Fig. 9," at various firing angle $\alpha$ of the inverter bridge. The efficiency and input-output powers can be given as in (22)-(25) below. The percentage efficiency of SRIM can be expressed as

$$\eta_1 = \frac{P_{out}}{P_{in} - P_{fb}} \times 100 \quad (20)$$

The Fourier block has been connected to measure the speed, rms value of current and power factor of the current. Discrete block has been connected in the circuit to measure the active and reactive power. The proposed model used a 2 hp, 415V, 50Hz, 1430 rpm SRIM for simulation and line commutated thyristors for the inverter bridge.

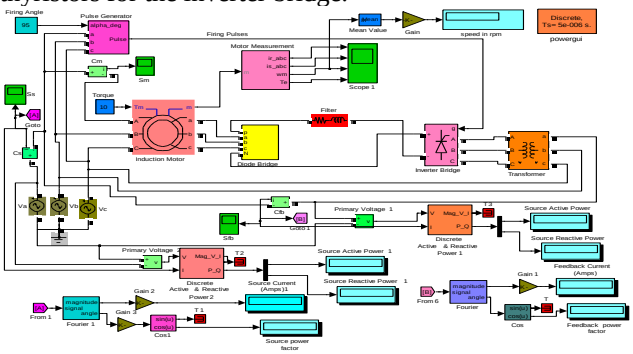

Fig. 3. Circuit Diagram of SPRS Employing Natural Commutated SCR Inverter

By running the model on MATLAB and varying the firing angle of inverter the speed and other observations have been plotted as shown in "Fig. 5,"- "Fig. 9,". The efficiency, output powers, and rotor speed are given by (21) - (23) below [18].
The efficiency (%) of the motor is given by:

$$\eta_1 = \frac{P_{out}}{P_{in} - P_{fb}} \times 100 \quad (21)$$

where, $\eta_1$ = the %age efficiency of IMD, $P_{in}$ = power input (W) and $P_{fb}$ = power feedback (W) are the power measured by the measurement blocks and $P_{out}$ = the mechanical power at the shaft (W) expressed as

$$P_{out} = \omega_r \times T_L \quad (22)$$

where $\omega_r$ is the rotor speed in rad/sec given as [20]

$$\omega_r = 2\pi \times \frac{N_r}{60} \quad (23)$$

where, $T_L$ = load torque in $Nm$, $N_r$ = rotor speed (rpm).

The proposed model of SPRS shown in "Fig. 4," using MOSFET chopper and inverter configuration is simulated in MATLAB. The speed of IMD is varied by varying duty-ratio of chopper (δ) from 80%-30% at an interval of 3% at fix value of inverter firing angle at 91°.The observed results of all the inverters configurations with MOSFET buck-boost chopper have been plotted as shown in "Fig. 10," – "Fig. 14,".

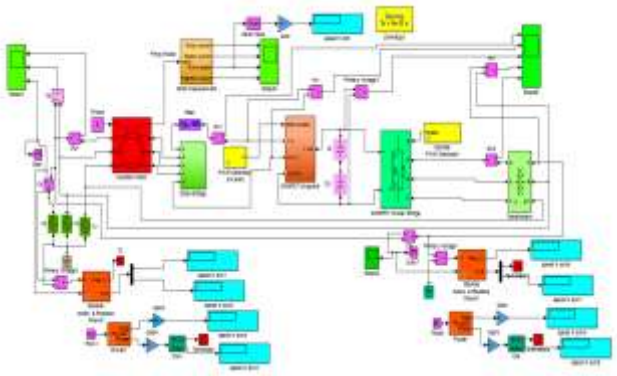

Fig. 4. Circuit Diagram of SPRS Employing MOSFET Based Buck-Boost Chopper and Inverter configuration

## IV. Results and Disscussion

The following simulation results have been obtained on MATLAB for IMD. The results of "Fig. 5,"–"Fig. 9," show the curves of IMD using SPRS with SCR inverter control technique.

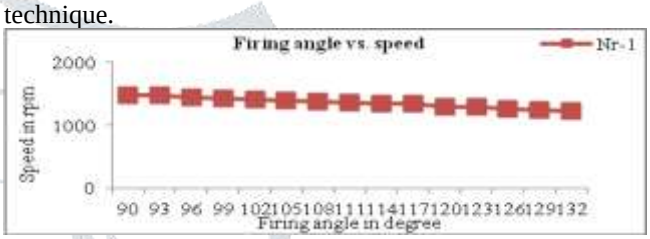


Fig. 5. Graph between firing angle and speed

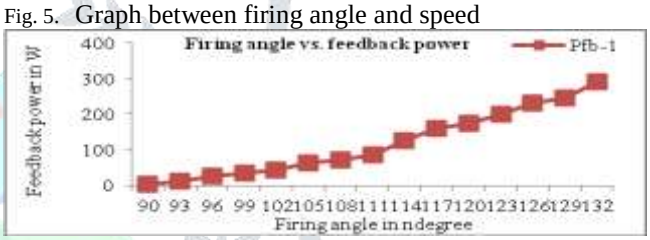


Fig. 6. Graph between firing angle and feedback power

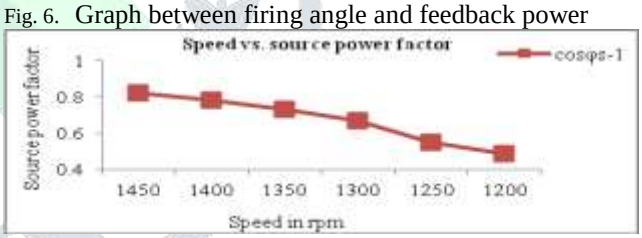


Fig. 7. Graph between speed and source power factor

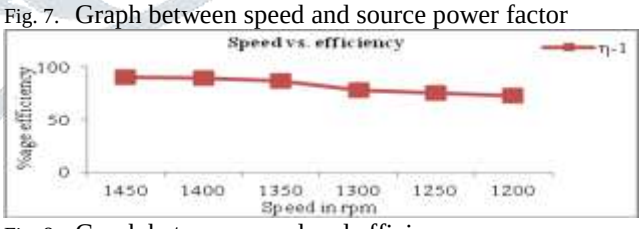


Fig. 8. Graph between speed and efficiency

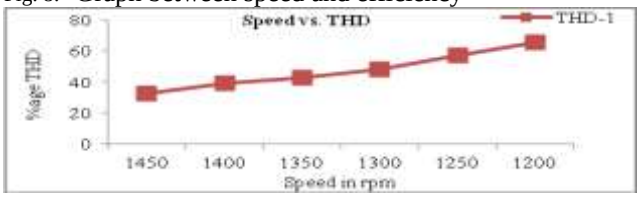


Fig. 9. Graph between speed and THD

### A. Firing angle vs. speed

Simulation has been carried for one second and constant of 8 Nm was applied to the IMD. The variations of speed by varying the firing angle obtained from simulations have been shown in "Fig. 5,". where the *Nr-1* indicates the rotor speed of induction motor with SCR inverter controller. The simulation

results have shown that with the increase in firing angle of inverter the rotor speed decreases and vice versa.

*B. Firing angle vs. feedback power*

Simulation results for inverter firing angle and feedback power have been shown in "Fig. 6," in which the $P_{fb-1}$ represents the feedback power. The result indicated that as the firing angle increases the feedback power also increases. For the constant load increase in feedback power, decreases the power drawn from the source consequently, enhance the efficiency of the drive.

*C. Speed vs. source power factor*

The graph of speed and source power factor has been shown in "Fig. 7," where the *cosφs-1* represents the source power factor. From the graph it is clear that there is decrease in source power factor with decrease in rotor speed. From the simulation results the average value of power factor is found to be 0.72.

*D. Speed vs. efficiency*

The graph of speed and efficiency has been shown in "Fig. 8," in which η-1 represent the efficiency of IMD. From the graph it is evident that with the decreases in rotor speed the efficiency of IMD also decreases. The average value of efficiency has been recorded as 84.3%. The increase in firing angle increases the feedback current which in turn increase the power loss in the feedback circuit hence slightly reduces the efficiency.

*E. Speed vs. THD*

"Fig. 9," shows the variations of the THD for different rotor speed where the *THD-1* indicating the THD of supply source. It has been observed from the graph that with the increase in firing angle or decrease in rotor speed, THD of the supply increases in case of inverter control. Because the increase in firing angle above 90° increases the reactive power consumption of inverter resulting in the increase in THD of the supply source.

The results of "Fig. 10," and "Fig. 11," show the curves of rotor speed and feedback power of IMD using SPRS with MOSFET chopper and PWM inverter control technique. The variations of source power factor, and THD w.r.t. speed have been shown in "Fig. 12,"– "Fig. 14,".

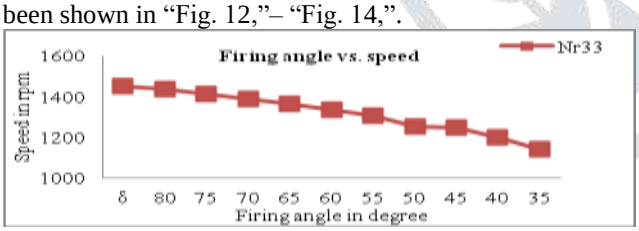


Fig. 10. Graph between duty ratio and speed

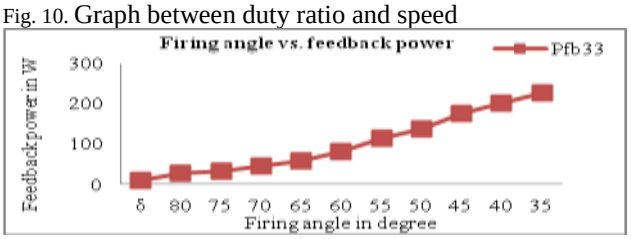


Fig. 11. Graph between duty ratio and feedback power

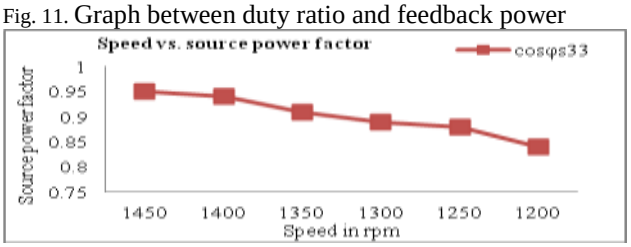


Fig. 12. Graph between duty ratio and source power factor

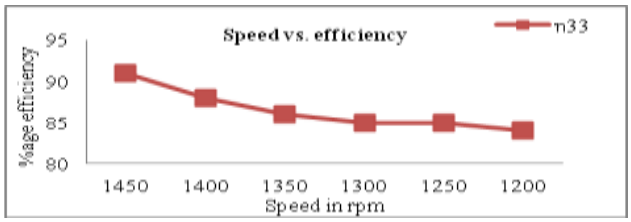


Fig. 13. Graph between duty ratio and efficiency

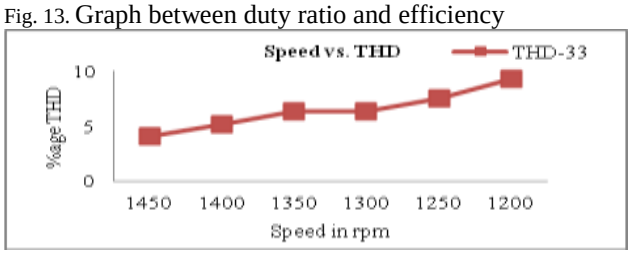


Fig. 14. Graph between duty ratio and THD

*F. Duty ratio vs. speed*

The graph of duty ratio and rotor speed $N_{r33}$ for MOSFET chopper and inverter configurations has been shown in "Fig. 10,", From these curves it has been observed that with the increase in duty ratio of chopper, the rotor speed increases and vice versa.

*G. Duty ratio vs. feedback power*

The variation of feedback power with respect to duty ratio has been shown in "Fig. 11," in which $P_{fb33}$ represent the feedback active power using MOSFET, chopper and inverter configuration. The feedback power increases with decrease in duty ratio of chopper, thereby decreases the speed. The rate of increment in feedback power shown by "Fig. 11," (duty ratio control) is more than by "Fig. 6," (firing angle control). Hence draw lees active power from the source resulting in better efficiency.

*H. Speed vs. source power factor*

The graph of duty ratio and source power factor is shown in "Fig. 12," where $cos\varphi_{s33}$ indicates the source power factor employing using MOSFET chopper and inverter configuration. From the graph it is seen that the source power factor slightly decreases with the decrease in duty ratio or speed.

*I. Speed vs. efficiency*

The graph between speed and efficiency has been shown in "Fig. 13,". Here the $\eta_{33}$ correspond to efficiency using MOSFET chopper and inverter configuration. From the graph it is seen that the efficiency increases as duty ratio or speed decreases because more power is feedback to the source.

*J. Speed vs. THD*

The variation of THD with respect to speed has been shown in "Fig. 14,". Here the $THD_{33}$ represents the THD of supply source using MOSFET chopper and inverter configuration. The THD of supply source increases with decrease in duty ratio of inverter or rotor speed.

The comparative curves of SPRS with MOSFET chopper and inverter configuration obtained from the simulations have been shown in "Fig. 15,"– "Fig. 17,". The results have been compared based on the equal speed range and load torque for IMD.

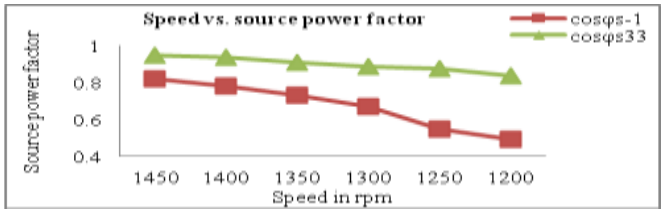


Fig. 15. Comparative graph of speed vs. source power factor

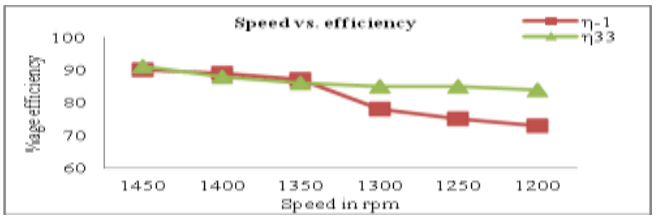


Fig. 16. Comparative graph of speedvs. efficiency

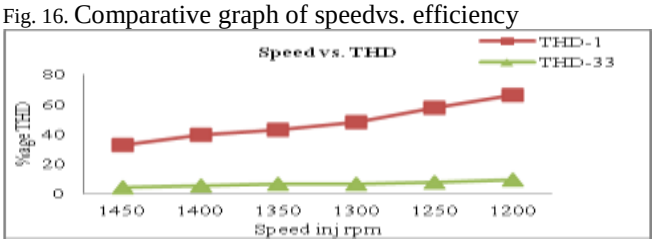


Fig. 17. Comparative graph of speed vs. THD

*K. Speed vs. source power factor*

"Fig. 15," shows the comparative graph of speed vs. source power factor employing SPRS with SCR inverter control and MOSFET chopper control techniques having the average values of power factors viz. 0.67 and 0.9 respectively. The power factor decreases in both the cases decreases however the rate of decrement in the chopper control method is less therefore has higher power factor with a margin of 34.3% than that of inverter control.

*L. Speed vs. efficiency*

"Fig. 16," shows the comparative graph of speed and efficiency of IMD using SPRS with SCR inverter control and MOSFET chopper control techniques having the average values of viz. 82 and 86.5 respectively. From the graph it is seen that the rate of decrease of efficiency has low in case of chopper control method. The chopper controller has higher average efficiency of 5.49% than inverter controller.

*M. Speed vs. THD*

"Fig. 16," shows the comparative graph of speed and efficiency of IMD using SPRS with SCR inverter control and MOSFET chopper control techniques having the average values of i.e. 42.63 and 6.46 respectively. The increase in THD is very less in comparision of inverter control method depicted in "Fig. 16,". Hence chopper control technique has reduced the THD by a margin of 49.8% that from the inverter control.

## V. Conclusions

The insvestigation of IMD has been proposed in this paper employing MOSFET chopper controlled SPRS with MOSFET PWMVSI. The proposed IMD has been simulated in MATLAB 2013b employing SCR inverter control and MOSFET chopper control with MOSFET inverter configuration. The power factor, efficiency and THD of source have been taken as parameters to examine the performance improvement of IMD. From the simulation results it has been observed that the chopper controller based SPRS has improved the source power factor and efficiency of IMD by a margin of 34.3% and 5.49% respectively and reduced the THD of the supply source by margin of 49.8% from the SCR inverter coltrol method. These results have suggested the application of SPRS using MOSFET chopper and PWMVSI control method for better performance of IMD than SCR inverter control method.

## References

[1] R. Ajabi-Farshba and M. R. Azizian, "Slip power recovery of induction machines using three-Level T -type converters," IEEE 5th Conference on Power Electronics, Drive Systems and Technologies, pp. 483-486, Feb 5-6, 2014.

[2] X. Yang, L. Xi, X. Yang, and Jian-guo Jiang, "Research on the application of PFC technology in cascade speed control system," IEEE 3rd Conference on Industrial Electronics and Applications ICIEA, pp. 1964-1969, 3-5 June, 2008.

[3] O. P. Rahi and A. K. Chandel, "Refurbishment and Uprating of Hydro Power Plants-A Literature Review," Renewable and Sustainable Energy Reviews, vol. 48, pp. 726-737, August 2015.

[4] O. P. Rahi and A. Kumar, "Economic Analysis for Refurbishment and Uprating of Hydro Power Plants," Renewable Energy, vol. 86, pp. 1197-1204, 2016.

[5] A. Lavi and R. J. Polge, "Induction motor speed control with static inverter in the rotor," IEEE Transaction on Power Apparatus and Systems, vol. PAS-85, pp. 76-84, 1966.

[6] W. Shepherd and J. Stanway, "Slip power recovery in an induction motor by the use of a thyristor inverter," IEEE Transactions on Industry and General Applications, vol. IGA-5, no. 1, pp. 74-82, 1969 .

[7] Sita Ram, O. P. Rahi, and Veena Sharma, "A comprehensive literature review on slip power recovery drives," Renewable and Sustainable Energy Reviews, vol. 73, pp. 922-934, 2017.

[8] P. Pilley and L. Refoufi, "Calculation of slip energy recovery induction motor drive behavior using the equivalent circuit," IEEE Transactions on Industry Applications, vol. 30, no. I. pp. 154-163, January/February 1994.

[9] G. D. Marques, "Numerical simulation method for the slip power recovery system," IEEE Proceedings of Electronic Power Application, vol. 146, no. 1, pp. 17-24, January 1999.

[10] G. D. Marques and P. Verdelho, "A simple slip-power recovery system with a dc voltage intermediate circuit and reduced harmonics on the mains," IEEE Transactions on Industry Electronics, vol. 47, no. 1, pp. 123-132, Feb. 2000.

[11] D. Panda, E. L. Benedict, G. Venkataramanan, and T. A. Lipo, "A novel control strategy for the rotor side control of a doubly-fed induction machine," IEEE Conference Record of 36th Annual meeting of Industry Applications, vol. 3, pp. 1695-1702, 30 September-4 October 2001.

[12] A. K. Mishra and A. K. Wahi, "Performance analysis and simulation of inverter fed slip -power recovery drive," IE (I) Journal-EL, vol. 85, pp. 89-95, Sept. 2004.

[13] S. Tunyasrirut, J. Ngamwiwita, V. Kinnares , T. Furuya, and Y. Yamamotod, "A DSP-based modified slip energy recovery drive using a 12-pulse converter and shunt chopper for a speed control system of a wound rotor induction motor," Electric Power Systems Research, vol. 78, no. 5, pp. 861–872, 2008.

[14] S. Tunyasrirut , V. Kinnares, and J. Ngamwiwit, "Performance improvement of slip energy recovery system by a voltage controlled technique," Renewable Energy, vol. 35, pp. 2235-2242, 2010.

[15] S. Tunyasrirut and V. Kinnares, "Speed and power control of a slip energy recovery drive using voltage-source PWM converter with current controlled technique," 10th Eco-Energy and Materials Science and Engineering Symposium, vol. 34, pp. 326-340, 2013.

[16] C. Pardhi, A. Yadavalli, S. Sharma, and G. A. Kumar, "A study of slip-power recovery schemes with a buck dc Voltage intermediate circuit and reduced harmonics on the mains by various PWM techniques," International Conference on Computation of Power, Energy, Information and Communication, pp. 495-499, 2014.

[17] S. Ram, O. P. Rahi, V. Sharma, and A. Kumar, "Performance analysis of slip power recovery scheme employing two inverter topologies," Proceedings of MFIIS, vol. 2, pp. 356-361, 12-13 September 2015.

[18] Sita Ram, O. P. Rahi and Veena Sharma, " Analysis of induction motor drive using buck-boost controlled slip power recovery scheme," IEEE International Conference on Power Electronics, Intelligent Control and Energy Systems, pp. 1985-1990, 4-6 July, 2016 DTU.

[19] G. K Dubey, "Fundamentals of Electrical Drives," 1995, Narosa Public House Delhi.

[20] N. Mohan, T. M. Undeleand, and W. P. Robbin, "Power electronics converters, aplications, and design." Third Edition, Willey India Pvt. Ltd. New Delhi 2014.